# Enhanced Carbon Monoxide Tolerance of Platinum Nanoparticles Synthesized through the Flash Joule Heating Method

J. Nandenha[a], L. Otubo[a], A.O. Neto[a], E. Antolini[b] and R.F.B. de Souza[a]

[a]Instituto de Pesquisas Energeticas e Nucleares, IPEN/CNEN-SP, Av. Prof. Lineu Prestes, 2242 Cidade Universitaria, CEP 05508-900, São Paulo, SP, Brazil
[b]Scuola Scienza Materiali, Via 25 aprile 22, 16016 Cogoleto, Genova, Italy

## Abstract:

Carbon supported Pt nanoparticles were synthesized by the Flash Joule Heating Method (FJHM). An aqueous solution of Pt precursor $H_2PtCl_6 \cdot 6H_2O$ was added to Vulcan XC 72 carbon into a reactor, and then this mixture was submitted to 50 cycles of discharges at 100 coulombs per discharge. Compared to a commercial Pt/C the X-ray Diffraction (XRD) analysis revealed an increase in the interplanar spacing of the platinum crystal lattice in the Pt/C catalyst prepared by FJHM, suggesting the emergence of structural defects. Transmission electronic microscopy (TEM) images showed distinct step-like features on the surface of FJHM-Pt/C, which may be indicative of structural defects, confirming X-ray Diffraction results. The cyclic voltammogram of the FJHM-Pt/C exhibited a significant increase in the oxidation pre-peak at 0.5 V compared to Pt/C BASF. Using pure $H_2$ as the fuel, the single proton exchange membrane fuel cell with the commercial Pt/C as the anode catalyst showed a higher maximum power density (MPD) than FJHM-Pt/C. In the presence of CO with $H_2$ the FJHM-Pt/C catalyst delivered a higher MPD compared to the cell with the commercial Pt/C. These results indicate an enhanced CO tolerance, underscoring the potential advantages of the FJHM preparation method.

**Keywords:** Pt electrocatalys; Flash Joule Heating Method; Carbon Monoxide, Fuel Cell, Cyclic Voltammetry

## Introduction

Polymer electrolyte membrane fuel cells (PEMFCs) are suitable tools for energy conversion, ascribed to their high power density, efficiency and operational viability at low temperatures. Platinum is commonly utilized as a catalyst at both the anode and cathode for the oxidation of hydrogen and the reduction of oxygen, respectively. $H_2$ is achieved primarily through catalytic reforming of hydrocarbons, leading to the common occurrence of carbon monoxide (CO). This impurityreduces the performance of $H_2$ at the anode due to its adsorption on the active sites of the platinum catalyst [1].

A potential strategy to mitigate the issue of CO adsorption on platinum surfaces involves the development of binary and ternary Pt-based catalysts, such as PtRu, PtMo and PtRuMo [2-7]. The presence of a second/third metal modifies the CO adsorption characteristics of Pt nanoparticles, this effect being attributed to either the electronic effect or the bifunctional mechanism. Alongside Pt, other metals such as Ir, Te, Cu, Fe, and Rh have been studied for this purpose [8-11].

A common method to prepare these electrocatalysts involves the utilization of sodium borohydride as a reducing agent for both Pt and the second/third metal precursors [12, 13]. Other method involves the process of spontaneous deposition of the second metal by immersing the platinum electrode within a solution that contains a ruthenium salt, leading to the irreversible adsorption of Ru onto the Pt surface [14]. In contrast, the forced deposition approach involves submerging the Pt electrode in an electrolyte under the presence of hydrogen bubbling or exposing the wet sample to a stream of $H_2$ gas [15]. This leads to the creation of a suitably reducing potential that promotes the direct deposition of Ru species onto the electrode. Both techniques predominantly employ Pt single-crystal surfaces as the preferred substrate [16].

Another approach entails the use of transition metal oxides, nitrides, carbides, or phosphides as co-catalysts. These co-catalysts serve to enhance the overall catalytic activity and selectivity of the Pt-based catalysts, particularly by influencing the adsorption properties of CO and other relevant species [17, 18].

Ramos et al. [11] reported a novel approach involving the utilization of a sodium borohydride reducing agent in conjunction with a magnetic field and radiofrequency pulse. This study revealed a compression of lattice strain within the Pt crystallographic structure. As a result, the adsorption energy of CO on Pt/C was potentially attenuated. This outcome might be attributed to the introduction of structural defects, suggesting a correlation between lattice strain manipulation and CO adsorption behavior. Li et al [19] showed that a Joule heating technique could induce the fragmentation of metal precursors, thereby facilitating the uniform blending of constituent elements. This is followed by a swift cooling phase, which facilitates the creation of precisely defined crystalline nanoparticles.

Qiu et al. [20] synthesized an Ag/Co/C electrocatalyst using the flash Joule heating method for the oxygen reduction reaction within an alkaline environment. Thishybrid catalyst delivereda specific activity that exceeded that of the pristine Ag/C by 40 times, and its mass activity surpassed the original by 52 times at 0.8 V vs. RHE in alkaline media. Additionally, the hybrid catalyst showed enhanced tolerance to methanol and ethanol compared to commercially available Pt/C electrocatalysts.

In the present work, for the first time a Pt/C electrocatalyst was prepared using the Flash Joule Heating process in a device developed within our research group. Theaim is to synthesize a catalyst with defects, thereby enhancing the activity for the oxidation of the $H_2$+CO mixture originating from catalytic reforming.

## Experimental

Pt/C 20% electrocatalyst was prepared using a Flash Joule Heating Method, a technique pioneered by our research team. which involves placing suitable quantities of the metal precursor $H_2PtCl_6.6H_2O$ (Aldrich), water in ratio of 1:1 (m/m)in relation of metal precursor and the Vulcan XC 72 carbon support into a graphite crucible. The crucible is subsequently sealed and subjected to 50 cycles of discharges at 100 coulombs per discharge at 65V, for a total time of 60 seconds. Subsequently, theobtainedFJHM - Pt/C catalyst was subjected to characterization.

The platinum load on carbon was determinedby thermogravimetric analysis performed on a SETARAM LABSYS. The samples were heated from 25 to 900 $^oC$ at aconstant rate of 10$^oC$ per minute.

The electrocatalysts were characterized through X-ray diffraction (XRD) utilizing a Rigaku Miniflex II diffractometer equipped with a Cu Kα source ($\lambda$ = 1.54056 Å) at a 2θ range spanning from 20° to 90°, employing a step size of 0.02° and a scan duration of 2 seconds per step. Transmission Electron Microscopy (TEM) analysis was carried out employing a JEOL electron microscope model JEM-2100.

Cyclic voltammetry measurements were carried outat a temperature of 25°C, employing an Autolab PGSTAT 302 potentiostat/galvanostat. The working electrode comprised a carbon vitreous material with a deposited porous ultrathin layer [21]. The reference electrode employed was the reversible hydrogen electrode (RHE), while the counter electrode took the form of a platinum (Pt) plate. These electrochemical analyses were performed within 0.5 mol $L^{-1}$ $H_2SO_4$ solutions saturated with nitrogen ($N_2$). For CO-stripping experiments, the working electrode was purged with $N_2$ for 30 minutes, then exposed to purified CO gas for an additional 30 minutes, with the working electrode potential set at 0.2 V vs. RHE. Following the adsorption process, CO was purged from the electrolyte solution, subsequently submitted to 15 minutes of $N_2$ bubbling. The CO-stripping voltammograms were recorded using a scan rate of 10 mV $s^{-1}$.

The fuel cell experiments were performed utilizing Pt/C materials synthesized by Flash Joule Heating Method for the anode and commercial Pt/C (BASF) for the cathode. A hydrogen flux of 300 mL $min^{-1}$ was employed for the anode, while the cathode utilized an oxygen flux of 200 mL $min^{-1}$. Tests were carried out in a single PEMFC, featuring electrodes with an active geometric surface area of 5.0 $cm^2$. The gas diffusion layer comprised PTFE-treated carbon cloth, and the electrolyte involved a Nafion® 117 membrane.

For the fuel cell investigations, both the anode and cathode utilized electrodes loaded with 1.0 $mg_{Pt}$ $cm^{-2}$ of electrocatalyst. In experiments involving the synthesis gas ($H_2$+CO), atmospheric pressure was maintained at the anode and cathode. The operating temperature of the fuel cell was set at 80°C, with the flux of $H_2$+CO (with CO at 100 ppm) regulated at 300 mL $min^{-1}$ for the anode, and $O_2$ flux set at 200 mL $min^{-1}$ for the cathode.

## Results and Discussion

As a novel synthesis method, the FJHM-Pt/C material was submitted to a thermographic analysis to verify the metal-to-carbon ratio. The weight loss of the electrocatalyst (Figure 1) initiates below 100°C as a result of the desorption of adsorbed water [22]. Noticeably, substantial mass reductions occur at approximately 230°C due to the decomposition and evolution of CO and $CO_2$ from the carbon support. After the depletion of carbon, the mass remained constant at 79.5%, indicating a platinum content of ~ 20%, and that during the synthesis there is no loss of carbon or platinum.

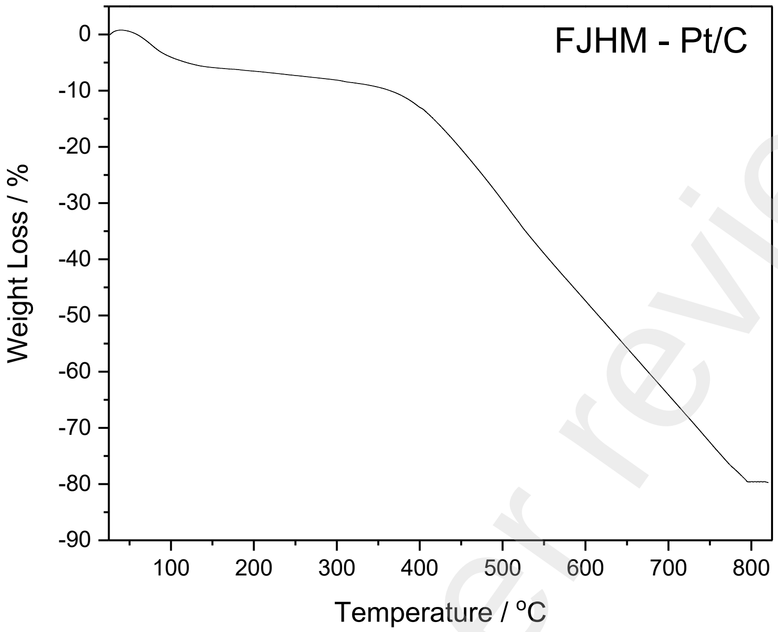

Figure 1: Thermogravimetric analysis of FJHM-Pt/C

The XRD patternsof FJHM-Pt/C and, for comparison, of a commercial Pt/C (BASF), prepared by a reduction-deposition method [22]areshownin Figure 2. The diffraction patterns revealed distinct peaks at 2θ angles of approximately 40°, 47°, 67°, 82°, and 86°, corresponding to the (111), (200), (220), and (311) planes of a face-centered cubic (FCC) structure. The Pt/C BASF sample aligned with the reference parameters JCPDS #87-647, featuring d-spacing values of 0.230, 0.194, 0.138, 0.117, and 112 nm for the (111), (200), (220), (311), and (222) planes, respectively.

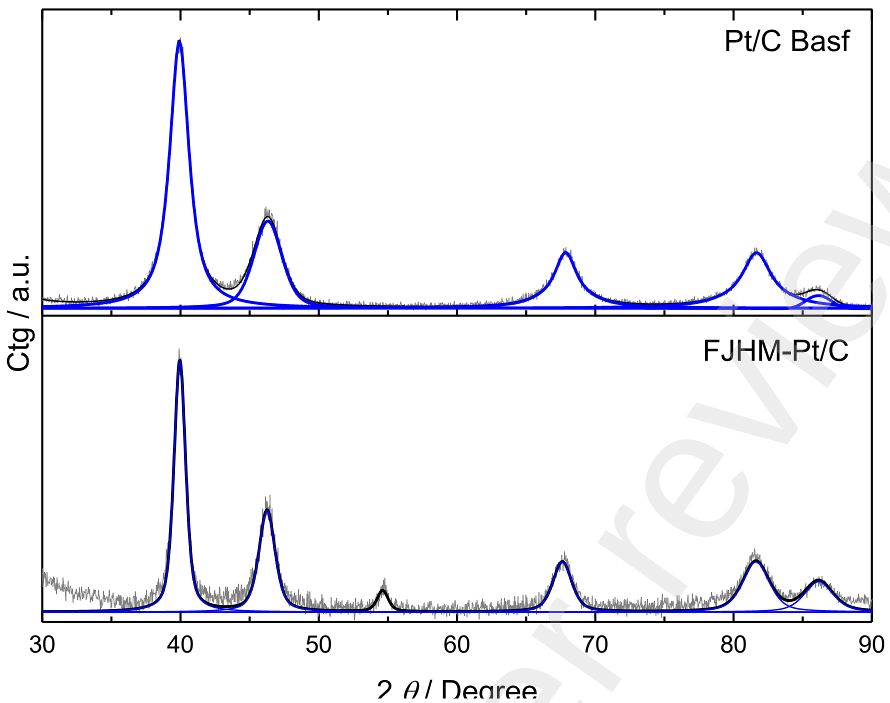

Figure 2. X-ray diffractions pattern of Pt/C BASF and FJHM-Pt/C.

In contrast, FJHM-Pt/C exhibited noticeable shifts toward more negative values in the 2θ angles for the (200), (220), (311), and (222) planes, while the (111) plane displays a shift towards more positive angles when compared to Pt/C BASF. This shift strongly suggests alterations in the lattice parameters of the crystal structure, with FJHM-Pt/C featuring d-spacing values of 0.224, 0.208, 0.142, 0.125, and 115 nm.

An additional significant observation was the prominence of the (222) plane peak, which appears considerably larger than that observed for the commercial Pt/C. To elucidate this, the relative intensities of the (111), (200), (220), (311), and (222) planes was calculated. In the case of commercial Pt/C, these planes showed relative intensities of 100, 42, 30, 28, and 5%, respectively, while for FJHM-Pt/C, the corresponding values were 100, 56, 32, 45, and 29%. This discrepancy indicates that the particle production method employed here discourages the formation of the (111) plane while favoring the high-index planes such as (311) and (222).These changes in the lattice parameters and relative plane intensities strongly suggest that the Flash Joule Heating method induced structural modifications in the platinum nanoparticles. Such structural alterations may lead to the emergence of structural defects, a phenomenon welldocumented in the literature, which has the potential to influence the catalytic properties of the material [23, 24].

Figure 3 displays transmission electron microscopy (TEM) images for both Pt/C BASF and FJHM-Pt/C. Both materials showed a well-dispersed distribution on the support. However, the particles in the FJHM-Pt/C catalyst were significantly larger in size and feature prominent corners, whereas the Pt/C BASF nanoparticles presented rounded shapes. The pronounced corners in the FJHM-Pt/C nanoparticles could be attributed to a rapid and forced reduction process induced by the electron cascade resulting from the discharges during synthesis.

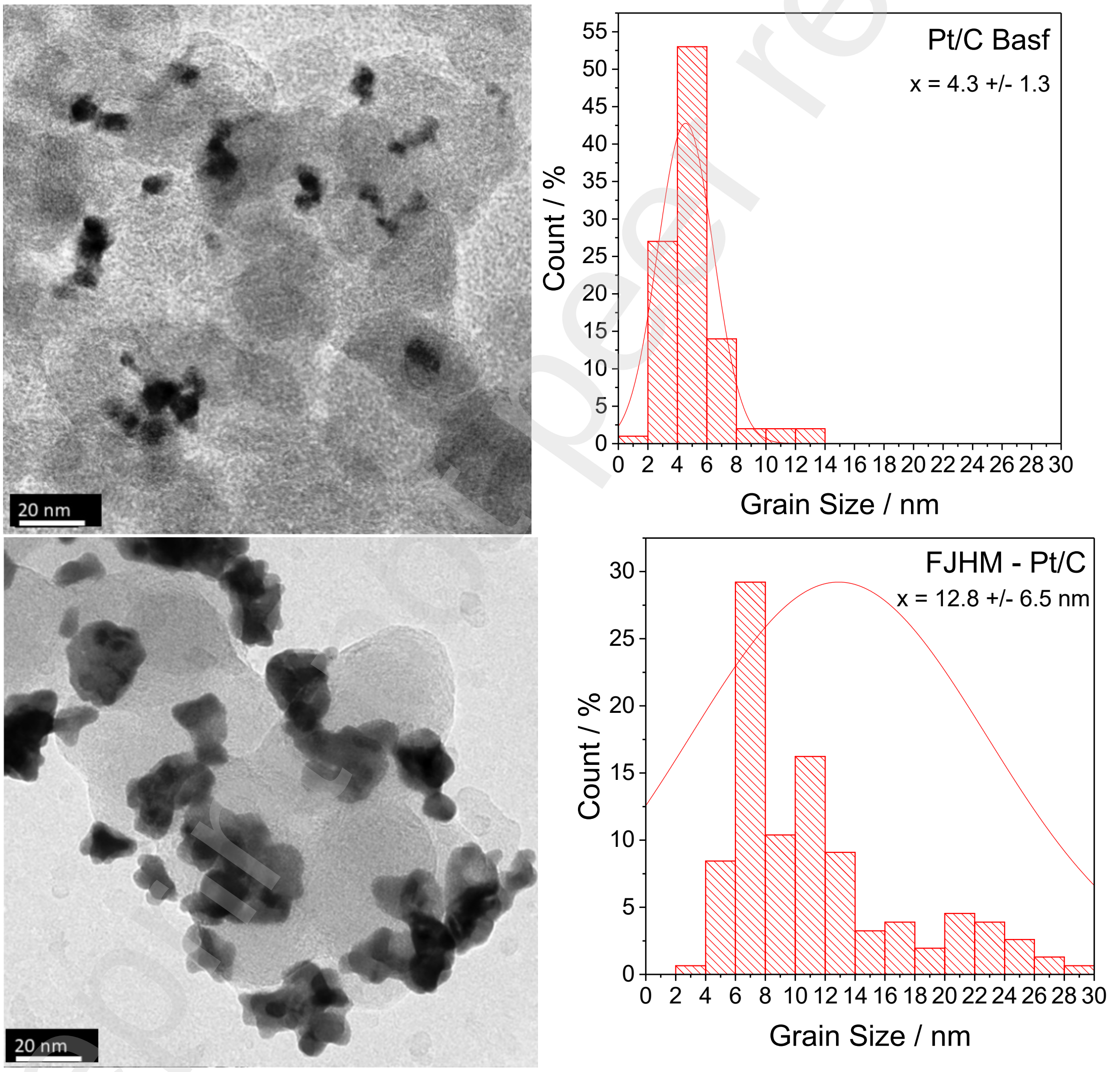

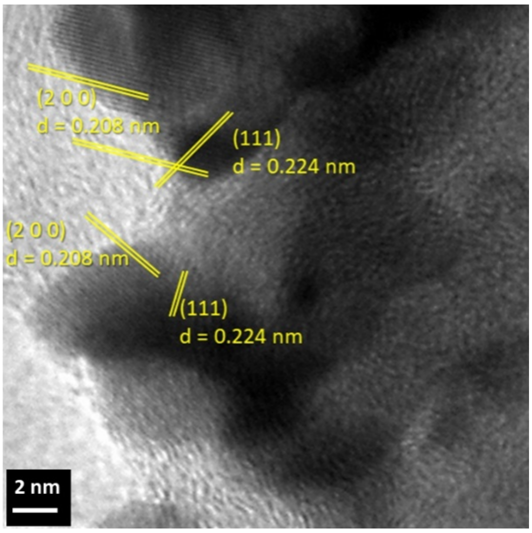

Figure 3. Transmission electron microscopy and nanoparticle size distribution of Pt/C BASF and FJHM-Pt/C.

Additionally, intriguingly, the TEM images of the FJHM-Pt/C catalyst revealed the presence of distinctive step-like features, which can be interpreted as indicative of defects within the crystal structure of the electrocatalyst. These findings prompt a more in-depth exploration of the impact of these structural differences on the electrocatalytic properties and performance of Pt/C in various applications.

Figure 4 shows the cyclic voltammetry of Pt/C BASF and FJHM-Pt/C nanoparticles during CO adsorption and desorption in a 0.5 mol $L^{-1}$ $H_2SO_4$ aqueous solution. In the absence of CO (depicted by the black line), a well-defined hydrogen adsorption and desorption region ranging from 0.05 to 0.4 V wasclearly observed [11, 22]. In the case of the FJHM-Pt/C catalyst, a reduction in the sharpness of the hydrogen adsorption and desorption peaks can be observed. This modification can be attributed to changes in the relative abundance of crystallographic facets or to defects generated during the particle formation process.

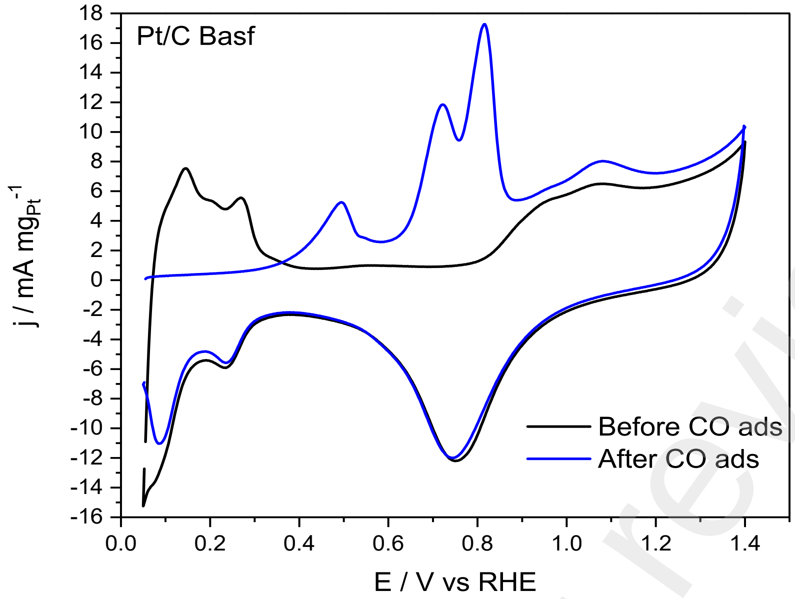

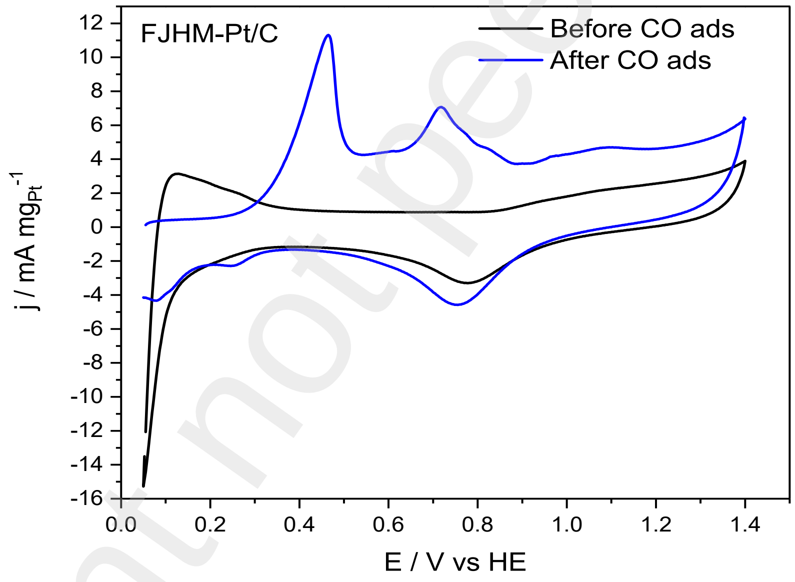

Figure 4. Cyclic voltammetry of Pt/C BASF and FJHM-Pt/C in 0.5 mol L$^{-1}$ $H_2SO_4$, v = 10 mV s$^{-1}$.

In the case of the commercial Pt/C and its CO oxidation behavior, it is possible to observe the typical pre-peak centered at 0.5 V, along with two additional higher peaks at 0.75 V and 0.85 V. However, when examining FJHM-Pt/C, a notably strong peak emerges at 0.45 V, which is significantly larger than that observed for Pt/C. Additionally, there are two less intense peaks at approximately 0.72 V and 0.82 V, corresponding to those observed for commercial Pt/C. This heightened peak at 0.45 V in

FJHM-Pt/C, when compared to Pt/C BASF, suggests that a substantial portion of the adsorbed intermediates has been oxidized at lower potential values. Cudero et al. [25, 26] have shown that the pre-peak corresponds to the oxidation of adsorbed CO, primarily resulting from its reaction with oxygenated species that initially nucleate at step sites. The appearance of the main peak coincides with the nucleation of oxygenated species not only at step sites but also on the terrace regions[26]. The presence of the pre-peak may also indicate an increase in structural defects within the electrocatalyst.

Figure 5 presents the polarization and power density curves for PEMFCs with both Pt/C BASF and FJHM-Pt/C as anode catalysts. In the case of pure $H_2$, the cell with the commercial Pt/C electrocatalyst showed a remarkable maximum power density (MPD) of approximately 32 mW $cm^2$ and an open-circuit potential of 0.85 V. Conversely, the cell with FJHM-Pt/C catalyst delivered a lower MPD of 22 mW $cm^2$, about 31% smaller than that of the cell with Pt/C BASF, and a reduced open-circuit potential to 0.75 V. These results emphasize the superior performance of the Pt BASF electrocatalyst for pure hydrogen oxidation, which can likely be attributed to its considerably smaller average particle size compared to FJHM-Pt/C.

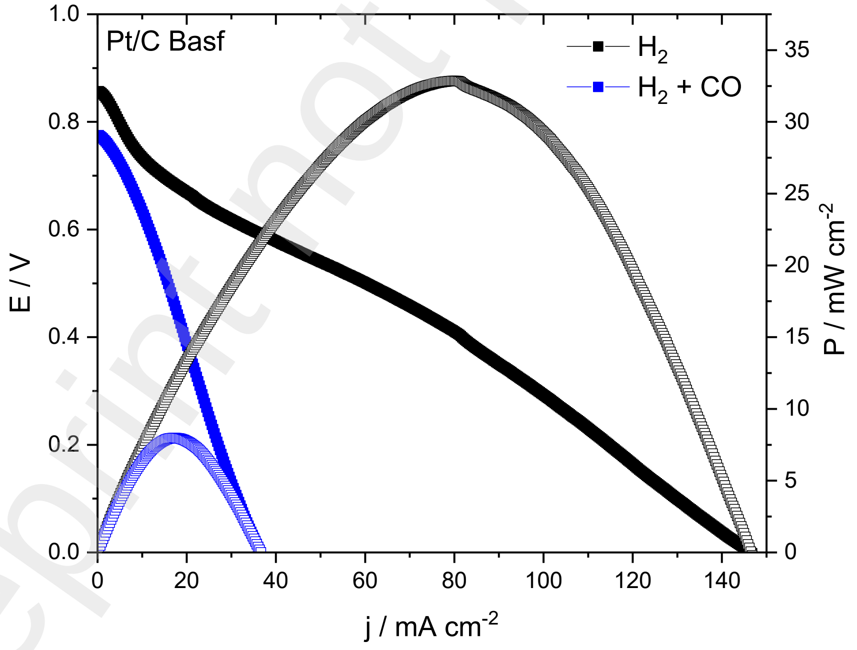

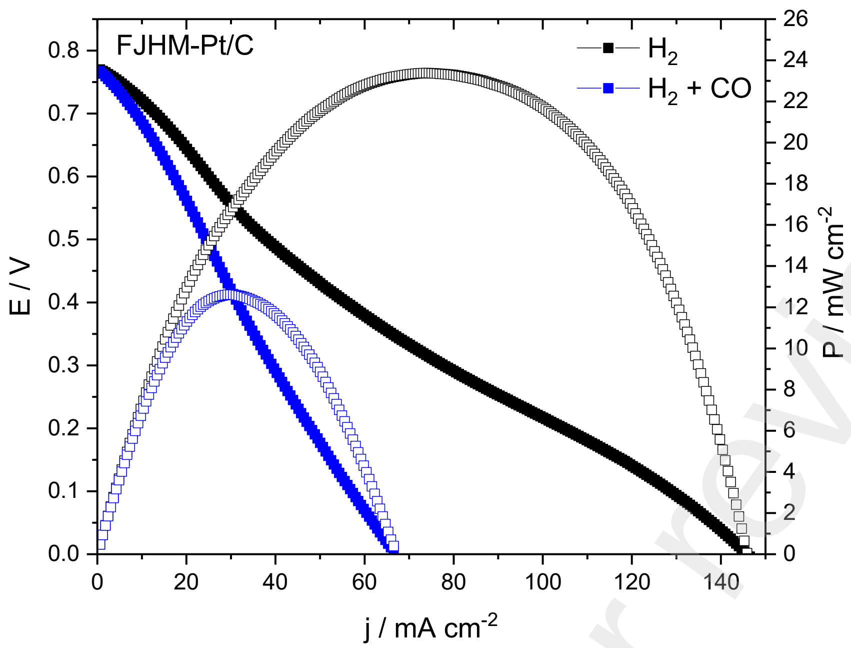

Figure 5. Polarization and power density curves for PEMFCs with Pt/C BASF and FJHM-Pt/C as the anode catalyst. The black lines represent the $H_2$ experiment and the blue lines $H_2$+CO experiment.

However, when the oxidation of an $H_2$+CO mixture in a single PEMFC was evaluated, an opposite result was observed. The FJHM-Pt/C electrocatalyst delivered a higher MPD (13.0 mW cm$^{-2}$) compared to the commercial Pt/C electrocatalyst (8.0 mW cm$^{-2}$). The reduction in maximum power density for the Pt/C BASF was approximately 75%, whereas for FJHM-Pt/C was46%. This suggests an improved tolerance to CO. This intriguing observation aligns with the cyclic voltammetry results. Several factors may contribute to this phenomenon, including the presence of surface defects, adlayers with varying crystallographic orientations, and/or strong metal/support interactions [11, 27-30]. These factors likely play a role in a complex, multi-step CO oxidation process on the Pt catalyst surface.

## Conclusion

The Flash Joule Heating Method enabled the preparation of an effective platinum electrocatalyst for the oxidation of the $H_2$+CO mixture. The thermographic analysis confirmed the metal load of 20%. X-ray diffraction revealed significant shifts in the diffraction angles for specific crystallographic planes in FJHM-Pt/C compared to Pt/C BASF. Notably, the (222) plane exhibited a more prominent peak in FJHM-Pt/C, suggesting a preference for high-index planes.TEM images further demonstrated that the FJHM-Pt/C particles were larger and featured prominent corners, while the commercial Pt/C particles had rounded shapes. Regarding CO oxidation behavior, FJHM-Pt/C exhibited a stronger peak at 0.45 V, indicating a higher ability for CO oxidation compared to Pt/C BASF. In single PEMFC tests with pure $H_2$, the commercial Pt/C outperformed FJHM-Pt/C, likely due to its smaller average particle size. However, in the presence of CO, the cell with the FJHM-Pt/C catalyst displayed a higher power density, indicating an enhanced CO tolerance. This result can be attributed to various factors, including Pt structural defects and metal-support interactions.

## Acknowledgements

We are grateful to CAPES, CNPq (350514/2023-2, 302709/2020-7) for financial support of this work.

## References

[1] Pei A, Ruan L, Liu B, Chen W, Lin S, Chen B, et al. Ultra-low Au decorated PtNi alloy nanoparticles on carbon for high-efficiency electro-oxidation of methanol and formic acid. International Journal of Hydrogen Energy. 2020;45:22893-905. https://doi.org/10.1016/j.ijhydene.2020.06.164
[2] Wee J-H, Lee K-Y. Overview of the development of CO-tolerant anode electrocatalysts for proton-exchange membrane fuel cells. Journal of Power Sources. 2006;157:128-35. https://doi.org/10.1016/j.jpowsour.2005.08.010
[3] Ioroi T, Akita T, Yamazaki S-i, Siroma Z, Fujiwara N, Yasuda K. Comparative study of carbon-supported Pt/Mo-oxide and PtRu for use as CO-tolerant anode catalysts. Electrochimica Acta. 2006;52:491-8. https://doi.org/10.1016/j.electacta.2006.05.030
[4] Hu JE, Liu Z, Eichhorn BW, Jackson GS. CO tolerance of nano-architectured Pt–Mo anode electrocatalysts for PEM fuel cells. International Journal of Hydrogen Energy. 2012;37:11268-75. https://doi.org/10.1016/j.ijhydene.2012.04.094
[5] Narischat N, Takeguchi T, Mori T, Iwamura S, Ogino I, Mukai SR, et al. Effect of the mesopores of carbon supports on the CO tolerance of Pt2Ru3 polymer electrolyte fuel cell anode catalyst. International Journal of Hydrogen Energy. 2016;41:13697-704. https://doi.org/10.1016/j.ijhydene.2016.05.272
[6] González-Hernández M, Antolini E, Perez J. Synthesis, Characterization and CO Tolerance Evaluation in PEMFCs of Pt2RuMo Electrocatalysts. Catalysts2019. 10.3390/catal9010061

[7] González-Hernández M, Antolini E, Perez J. CO tolerance and stability of PtRu and PtRuMo electrocatalysts supported on N-doped graphene nanoplatelets for polymer electrolyte membrane fuel cells. International Journal of Hydrogen Energy. 2020;45:5276-84. https://doi.org/10.1016/j.ijhydene.2019.05.208
[8] Yang X, Wang Y, Wang X, Mei B, Luo E, Li Y, et al. CO-Tolerant PEMFC Anodes Enabled by Synergistic Catalysis between Iridium Single-Atom Sites and Nanoparticles. Angewandte Chemie International Edition. 2021;60:26177-83. https://doi.org/10.1002/anie.202110900
[9] Brkovic SM, Marceta Kaninski MP, Lausevic PZ, Saponjic AB, Radulovic AM, Rakic AA, et al. Non-stoichiometric tungsten-carbide-oxide-supported Pt–Ru anode catalysts for PEM fuel cells – From basic electrochemistry to fuel cell performance. International Journal of Hydrogen Energy. 2020;45:13929-38. https://doi.org/10.1016/j.ijhydene.2020.03.086
[10] Sarma PJ, Gardner CL, Chugh S, Sharma A, Kjeang E. Strategic implementation of pulsed oxidation for mitigation of CO poisoning in polymer electrolyte fuel cells. Journal of Power Sources. 2020;468:228352. https://doi.org/10.1016/j.jpowsour.2020.228352
[11] Ramos AS, Santos MCL, Godoi CM, de Queiroz LC, Nandenha J, Fontes EH, et al. High CO tolerance of Pt nanoparticles synthesized by sodium borohydride in a time-domain NMR spectrometer. International Journal of Hydrogen Energy. 2020;45:22973-8. https://doi.org/10.1016/j.ijhydene.2020.06.105
[12] Silva JCM, Ntais S, Rajaraman V, Teixeira-Neto É, Teixeira-Neto ÂA, Neto AO, et al. The Catalytic Activity of Pt:Ru Nanoparticles for Ethylene Glycol and Ethanol Electrooxidation in a Direct Alcohol Fuel Cell. Electrocatalysis. 2019;10:203-13. 10.1007/s12678-019-00515-8
[13] Silva JCM, Ntais S, Teixeira-Neto É, Spinacé EV, Cui X, Neto AO, et al. Evaluation of carbon supported platinum–ruthenium nanoparticles for ammonia electro-oxidation: Combined fuel cell and electrochemical approach. International Journal of Hydrogen Energy. 2017;42:193-201. https://doi.org/10.1016/j.ijhydene.2016.09.135
[14] Maillard F, Lu GQ, Wieckowski A, Stimming U. Ru-Decorated Pt Surfaces as Model Fuel Cell Electrocatalysts for CO Electrooxidation. The Journal of Physical Chemistry B. 2005;109:16230-43. 10.1021/jp052277x
[15] Beck A, Frey H, Becker M, Artiglia L, Willinger MG, van Bokhoven JA. Influence of Hydrogen Pressure on the Structure of Platinum–Titania Catalysts. The Journal of Physical Chemistry C. 2021;125:22531-8. 10.1021/acs.jpcc.1c05939
[16] Caballero-Manrique G, Brillas E, Centellas F, Garrido JA, Rodríguez RM, Cabot P-L. Electrochemical Oxidation of the Carbon Support to Synthesize Pt(Cu) and Pt-Ru(Cu) Core-Shell Electrocatalysts for Low-Temperature Fuel Cells. Catalysts2015. p. 815-37. 10.3390/catal5020815
[17] Molochas C, Tsiakaras P. Carbon Monoxide Tolerant Pt-Based Electrocatalysts for H2-PEMFC Applications: Current Progress and Challenges. Catalysts2021. 10.3390/catal11091127
[18] Fontes EH, Ramos CED, Nandenha J, Piasentin RM, Neto AO, Landers R. Structural analysis of PdRh/C and PdSn/C and its use as electrocatalysts for ethanol oxidation in alkaline medium. International Journal of Hydrogen Energy. 2019;44:937-51. https://doi.org/10.1016/j.ijhydene.2018.11.049
[19] Li J, Wang C, Chen X, Zhang Y, Zhang Y, Fan K, et al. Flash synthesis of ultrafine and active NiRu alloy nanoparticles on N-rich carbon nanotubes via joule heating for efficient hydrogen and oxygen evolution reaction. Journal of Alloys and Compounds. 2023;959:170571. https://doi.org/10.1016/j.jallcom.2023.170571

[20] Qiu Y, Hu Z, Li H, Ren Q, Chen Y, Hu S. Hybrid electrocatalyst Ag/Co/C via flash Joule heating for oxygen reduction reaction in alkaline media. Chemical Engineering Journal. 2022;430:132769. https://doi.org/10.1016/j.cej.2021.132769
[21] De Souza RFB, Neto ÉT, Calegaro ML, Santos EA, Martinho HS, dos Santos MC. Ethanol Electro-oxidation on Pt/C Electrocatalysts: An "In Situ" Raman Spectroelectrochemical Study. Electrocatalysis. 2011;2:28-34. 10.1007/s12678-010-0031-0
[22] Qiu J-D, Wang G-C, Liang R-P, Xia X-H, Yu H-W. Controllable Deposition of Platinum Nanoparticles on Graphene As an Electrocatalyst for Direct Methanol Fuel Cells. The Journal of Physical Chemistry C. 2011;115:15639-45. 10.1021/jp200580u
[23] Şen F, Gökağaç G. Activity of Carbon-Supported Platinum Nanoparticles toward Methanol Oxidation Reaction: Role of Metal Precursor and a New Surfactant, tert-Octanethiol. The Journal of Physical Chemistry C. 2007;111:1467-73. 10.1021/jp065809y
[24] Cui H-F, Ye J-S, Zhang W-D, Wang J, Sheu F-S. Electrocatalytic reduction of oxygen by a platinum nanoparticle/carbon nanotube composite electrode. Journal of Electroanalytical Chemistry. 2005;577:295-302. https://doi.org/10.1016/j.jelechem.2004.12.004
[25] López-Cudero A, Cuesta Á, Gutiérrez C. Potential dependence of the saturation CO coverage of Pt electrodes: The origin of the pre-peak in CO-stripping voltammograms. Part 2: Pt(100). Journal of Electroanalytical Chemistry. 2006;586:204-16. https://doi.org/10.1016/j.jelechem.2005.10.003
[26] Cuesta A, Couto A, Rincón A, Pérez MC, López-Cudero A, Gutiérrez C. Potential dependence of the saturation CO coverage of Pt electrodes: The origin of the pre-peak in CO-stripping voltammograms. Part 3: Pt(poly). Journal of Electroanalytical Chemistry. 2006;586:184-95. https://doi.org/10.1016/j.jelechem.2005.10.006
[27] García G, Koper MTM. Stripping voltammetry of carbon monoxide oxidation on stepped platinum single-crystal electrodes in alkaline solution. Physical Chemistry Chemical Physics. 2008;10:3802-11. 10.1039/B803503M
[28] Ji W, Qi W, Tang S, Peng H, Li S. Hydrothermal Synthesis of Ultrasmall Pt Nanoparticles as Highly Active Electrocatalysts for Methanol Oxidation. Nanomaterials2015. p. 2203-11. 10.3390/nano5042203
[29] Farias MJS, Cheuquepan W, Camara GA, Feliu JM. Disentangling Catalytic Activity at Terrace and Step Sites on Selectively Ru-Modified Well-Ordered Pt Surfaces Probed by CO Electro-oxidation. ACS Catalysis. 2016;6:2997-3007. 10.1021/acscatal.6b00439
[30] Luo W, Jiang Y, Wang M, Lu D, Sun X, Zhang H. Design strategies of Pt-based electrocatalysts and tolerance strategies in fuel cells: a review. RSC Advances. 2023;13:4803-22. 10.1039/D2RA07644F